

AO12: Empirical methods for detecting atmospheric aerosol events from satellite measurements

Candidate number: 45107

Supervisors: Dr. G. Thomas, Dr. R. G. Grainger

Word count: 6556

Abstract

Aerosols have an important influence on the climate directly, through scattering and absorption of radiation, and indirectly by affecting cloud formation. The Oxford-RAL Aerosol and Cloud aerosol retrieval aims to use data from satellites (AATSR and ATSR-2) to increase understanding of aerosol properties and their impacts. Clouds must be eliminated from the data prior to processing to prevent contamination but the clearing system often also removes large aerosol events important to aerosol research. This project investigates methods to create a flagging system for large aerosol events to include volcanic ash, desert dust and smoke from biomass burning in order to distinguish them from cloud and allow their inclusion in the ORAC retrieval process.

1 Introduction

1.1 Importance of aerosols

Aerosols are defined as a dispersion of liquid or solid particles that are suspended in gas. There are many sources of which a significant number are natural, but there is also an increasing contribution from human activity. It can be challenging to study aerosols and to understand their impacts due to their great variability in size, length of time in the atmosphere and the distance over which they can travel.

Aerosols have effects on two important atmospheric processes. Firstly, the particles play a significant role in absorbing and scattering sunlight or thermal radiation from the ground be-

low. Aerosols often have an overall cooling effect, counteracting the increase in temperatures of global warming. The local heating and cooling may affect synoptic patterns and consequently humidity, temperature and precipitation [13]. Secondly, aerosols influence cloud formation either through their impacts on the radiation or by acting as nucleation sites for cloud droplets. Currently, the evolution of cloud in climate change prediction and climate modelling remains a large uncertainty [15] and understanding the affects of aerosols on clouds may increase the reliability of predictions.

1.2 AATSR

Much of the technical information about the instruments mentioned in this section has been obtained from [6] and [4]. Further information can also be found in Appendix A.

The Advanced Along Track Scanning Radiometer (AATSR), operational in 2002, and a previous generation Along Track Scanning Radiometer, ATSR-2, provide global measurements that can be used to retrieve, for example, sea surface temperatures. Both instruments have seven spectral channels - four in the visible range and three in the infrared - as shown in table 1. They are dual view radiometers with one aperture directed in the nadir view and the second, forward view at a viewing angle of 55° to the nadir looking at the surface approximately 900 km ahead of the satellite. Though not simultaneous, the same area is viewed by the multiple views with a very short delay of around 150 s.

Data from AATSR was used throughout this

study, however the flags developed in this project should also be applicable to ATSR-2 data.

Channel	Central wavelength	Width of band	Output
0.55	0.555 μm	20nm	R
0.66	0.659 μm	20nm	R
0.87	0.865 μm	20nm	R
1.6	1.61 μm	0.3 μm	R
3.7	3.70 μm	0.3 μm	BT
11.0	10.85 μm	1.0 μm	BT
12.0	12.00 μm	1.0 μm	BT

Table 1: Spectral channels of AATSR
R = Radiance, BT = Brightness temperature

1.3 ORAC aerosol retrieval and cloud flagging

The Oxford-RAL Aerosol and Cloud aerosol retrieval [18] uses the multiple views of the (A)ATSR instruments to derive atmospheric aerosol properties, in particular the aerosol optical depth. A key element of the retrieval is the inclusion of *a priori* data - an estimation of the retrieval parameters before any direct measurement - to produce more accurate results.

Before the retrieval can be made, cloud must be removed to prevent contamination of results. This is carried out through a series of tests provided by the European Space Agency, ESA (who supply the AATSR data) which are applied in both the nadir and forward views. Unfortunately, large aerosol events such as plumes of volcanic ash are sometimes mistakenly flagged as cloud so that these significant regions of aerosol are not included in the ORAC retrieval. Further information about the retrieval process and the cloud flagging can be found in Appendix B.

This report discusses empirical methods to create a flagging system to distinguish cloud from these large events, focussing on volcanic ash, desert dust and smoke from biomass burning. A successful flag for each type of aerosol should locate the dense regions of particles and produce as few as possible false results elsewhere. Areas determined to be aerosol will then be included in the retrieval and information about the aerosol type can be added to the *a priori* data.

2 Aerosol properties and existing aerosol flags

There are two main characteristics of aerosols that influence the radiation measured - the way in which the particles scatter the radiation and the composition of the aerosol which may contain distinctive absorption features. When examining the scattering an important property to consider is the size parameter defined as:

$$x = \frac{2\pi r}{\lambda} \quad (1)$$

where r is the radius of the particle and λ is the wavelength of the incoming radiation. If $x \ll 1$, in the case of small r or large λ , then Rayleigh scattering results - a more uniform scattering of radiation with slightly greater intensity in the forward and backward directions. For $x \gtrsim 1$, Mie scattering occurs where there is a distinct direction in which the radiation is scattered, enhancing the signal at that wavelength in the forward scattering direction. The transition from the Rayleigh to the Mie regime is quite rapid, leading to a rapid increase in the scattered intensity with increasing x . Hence, smaller aerosol particles have little effect on the thermal channels and for a given wavelength larger particles will have a larger impact than smaller particles.

There have been some flags already developed for aerosol detection using data from other instruments. Frequently the tests require data from wavelengths that AATSR does not possess but there are also some widely used methods that could be applied. In order to develop flags tailored to the AATSR data, existing tests are investigated and adapted as appropriate. For the three aerosol types considered here, it is often acknowledged that detection can be made more difficult by the evolution of the particle properties with age (e.g. Prata, 1989 [16]). Thin layers of aerosol or mixing with water/ice cloud can also make flagging more problematic as the spectral contrasts may become less pronounced.

2.1 Volcanic ash

Volcanic ash particles tend to be quite large and so fall into the Mie regime of scattering for most

of the AATSR wavelengths. This means that the particles are likely to still have significant impact on the longer wavelength channels. Volcanic ash is composed mostly of siliceous material derived from acidic rocks in explosive eruptions or basaltic rocks in less explosive eruptions [16]. Often large amounts of SO_2 are also released which may be hydrated and oxidized to form H_2SO_4 . It has been shown that acidic siliceous rocks have a lower emissivity at $11.0\mu\text{m}$ than at $12.0\mu\text{m}$, with the minimum lying between $8.0\mu\text{m}$ and $9.7\mu\text{m}$. Similarly H_2SO_4 shows a stronger absorption at $11.0\mu\text{m}$ than at $12.0\mu\text{m}$ as well. Conversely, for water/ice the emissivity is found to be higher at $11.0\mu\text{m}$ [16], [9].

In previous studies, volcanic ash has successfully been detected using a test that considers the brightness temperature (BT) difference between $11.0\mu\text{m}$ and $12.0\mu\text{m}$. A negative difference between the two wavelengths, which is rarely seen for water/ice cloud, is used to signify ash [16] – this is known as the ‘split-window’ test. Tests have also included use of the BT difference between around $8.0\mu\text{m}$ and $12.0\mu\text{m}$ [10] since the absorption feature is strong near $8.0\mu\text{m}$, but there is no equivalent channel near $8.0\mu\text{m}$ for AATSR.

The $3.7\mu\text{m}$ channel has strong components of both the solar radiation and radiation from the Earth’s surface. Smaller droplets or ice particles better scatter the shorter wavelength radiation as the reflectance at shorter wavelengths is inversely proportional to the cloud droplet size [10]. Samples of volcanic ash have also shown a higher reflectance around $3.7\mu\text{m}$ than at $11.0\mu\text{m}$ or $12.0\mu\text{m}$ [10]. However, the potential confusion with small water/ice particles means that a test involving the BT difference between $3.7\mu\text{m}$ and $11.0\mu\text{m}$ or $12.0\mu\text{m}$ may not alone be able to isolate the ash.

The following combination of tests, applied previously to data from the Spinning Enhanced Visible and InfraRed Imager (SEVIRI), uses wavelengths known to be useful in volcanic ash detection [5]. The first part combines the $11/12\mu\text{m}$ and $11/3.7\mu\text{m}$ differences with numerical factors. The second part requires the radiance in the $0.66\mu\text{m}$ channel to be below a certain

value. The final part uses a Normalised Difference Vegetation Index (NDVI) test defined as:

$$\text{NDVI} = \frac{(R_{0.55} - R_{0.66})}{(R_{0.55} + R_{0.66})} \quad (2)$$

As the wavelength becomes shorter the absorption of the ash increases leading to a lower radiances. This means that the NDVI should reveal negative results unlike clouds which tend to scatter the light more uniformly, leading to smaller negative differences often being observed [14].

2.2 Desert dust

As with volcanic ash, desert dust particles tend to be relatively large, for instance in comparison to smoke from biomass burning or background aerosol. This implies that they will also cause Mie scattering rather than Rayleigh scattering in most, if not all, of the channels of AATSR. Dust particles also have a siliceous composition [11] so that, like volcanic ash, the BT should increase between $11.0\mu\text{m}$ and $12.0\mu\text{m}$. This leads to a negative difference between $11.0\mu\text{m}$ and $12.0\mu\text{m}$ being used to indicate dust as well. Similarly, higher reflectances are also observed for dust at $3.7\mu\text{m}$ than at $11.0\mu\text{m}$ or $12.0\mu\text{m}$ [10]. Hence the BT difference between $3.7\mu\text{m}$ and $11.0\mu\text{m}$ or $12.0\mu\text{m}$ has also been tried in dust detection but ambiguity arises again with clouds composed of small water/ice particles. A test considering the difference between a channels at around $8\mu\text{m}$ and $12\mu\text{m}$, which is unfortunately unavailable using AATSR data, has also been implemented with some success.

A dust detection scheme designed for Moderate Resolution Imaging Spectroradiometer (MODIS) [14] uses a combination of tests and notes that different strategies were required for land and sea. The split-window test is used over both surfaces although there is some concern that some land surfaces can produce signatures difficult to distinguish from airborne dust. A second test over both land and sea utilizes the colour of the dust. At visible wavelengths, the complex part of the imaginary refractive index of mineral dust increases with decreasing wavelength. This results in the dust absorbing more at the

short wavelengths. A Normalized Dust Difference Index (NDDI) between $0.67\mu\text{m}$ and $0.44\mu\text{m}$ identifies the dust by large positive differences. The cloud, which scatters all visible wavelengths more uniformly, tends to have small positive differences. The normalization enables better detection of weaker signals. However, while using NDDI is effective over water, over land the surface is also enhanced making dust much more difficult to distinguish. For further verification of dust over land, the MODIS scheme also considers that lofted dust will have cooled to the temperature of its surrounding in the atmosphere so that it appears cooler than the surface in the infrared channels.

Miller, 2003 [14] and Brindley *et. al*, 2006 [8] suggest the use of a test exploiting the spatial properties of blowing dust. Dust tends to extend uniformly over relatively large areas in contrast to cloud which is usually more variable (although thin cirrus clouds can sometimes appear similar). Brindley *et. al*, 2006 [8] suggests to consider $27 \times 27 \text{ km}^2$ boxes of pixels stepping pixel by pixel across the image. If more than 60% of the pixels in the box are flagged as dust then the central pixel is flagged as dust otherwise it is considered to be cloud and assigned a negative result.

Brindley *et. al*, 2006 [8] also noted that as the dust layer varies with altitude the relative spectral behaviour does not change significantly unless near large temperature inversion where the emitting temperature is higher than the surface beneath.

2.3 Smoke from biomass burning

The optical properties of smoke from biomass burning vary due to differences in fuel type and combustion conditions. The optical properties depend on particle size, shape and black carbon (formed from incomplete combustion) content or brown carbon (formed later, once in the atmosphere) content. The carbonaceous aerosols tend to have the greatest impact on the radiation [1]. The age of the smoke may also cause properties to change as the particles react in the atmosphere [2]. Smoke consists of mostly fine particles and particularly affects the ultraviolet

part of the spectrum as black and brown carbon are increasingly absorptive towards shorter wavelengths with little effect in the infrared regions (for brown carbon, the peak in absorption is in the near-ultraviolet region). This also links with the type of scattering as the wavelength increases - the small smoke particles will mostly be in the Rayleigh regime for the longer wavelength channels of AATSR, reducing their impact.

Hutchinson *et. al*, 2007 [12] exploited the properties described above by using a ratio between channels at $0.412\mu\text{m}$ and $2.2\mu\text{m}$ to test for smoke using data from The National Polar-orbiting Operational Environmental Satellite System (NPOESS). Since at the longer wavelength, the aerosol should be more transmissive, this ratio should be small for smoke. However, it was noted that ice clouds can be misidentified with this test.

Smoke tends to have relatively uniform properties across the plume at any particular time. Similar to desert dust, a form of spatial test has also been suggested for detection of smoke [3] but using smaller box sizes of 9×9 pixels with spatial resolution of 1.1 km. Tests also included a lower limit set on an infrared channel to try to distinguish between, in particular, the colder cloud at greater altitudes and the warm smoke generally found at lower altitudes. Further to this, with knowledge of the increasing transmittance towards longer wavelengths, Asakuma *et. al*, 2002 [3] uses the normalized difference between images in $0.58\text{-}0.68\mu\text{m}$ and $10.3\text{-}11.3\mu\text{m}$ to highlight the smoke. Values above a particular threshold (set empirically) indicate a positive result.

3 Development of the aerosol flags

Initially, any applicable tests found in the literature, as detailed in Section 2, were trialled on the AATSR data. If these did not produce an effective flagging system then further tests were devised from knowledge of the properties of the particle. Combinations of tests were required for each aerosol type since it was difficult to set a

threshold on one test alone that would successfully detect the aerosol and produce few false positive readings. In all cases, thresholds were set empirically which led to the method being an iterative process where the limits placed on the tests were refined as new examples of the aerosol were analysed or in reducing false positive results. If a pixel is flagged as positive for a certain aerosol, it is assigned the value ‘1’ and all other pixels are given the value ‘0’.

A colour image was constructed using $0.66\mu\text{m}$ as the red channel, $0.87\mu\text{m}$ as the green channel and $0.55\mu\text{m}$ as the blue channel. This allowed the causes of features observed in the images of different channels/channel combinations used in the tests to be verified. It was also used to gauge the extent to which flagged pixels covered the region of aerosol. Where possible, plots were constructed of the pixel values for different tests for all the pixels in the image to find out whether the aerosol had distinct values. The $11.0\mu\text{m}$ channel could also be used to aid in locating clouds due to their cold temperatures when they reach higher altitudes.

To investigate the level of false readings that each flagging system would produce, initially a selection of different surfaces were tested. Each flag for a particular aerosol was applied, where possible, on the other types of aerosol investigated in this project. Areas of hot land around the Equator and Australia, warm sea off the coast of Africa and colder land and sea around Alaska were analysed. The effectiveness of each flag was also considered over areas of ice and cold water in the Antarctic and across Europe, including the Alps. However, for a more reliable estimate of how well the flags worked they were subsequently applied to many orbits of data spanning several days. The results of this are examined in Section 4 while in this section discussion of control testing will refer to the small selection of areas listed above.

3.1 Volcanic ash

A volcanic eruption occurred on 28/10/2002 from Mt. Etna, Sicily, and the resulting plume in the region $30\text{--}40^\circ\text{N}$, $8\text{--}16^\circ\text{E}$ was selected for

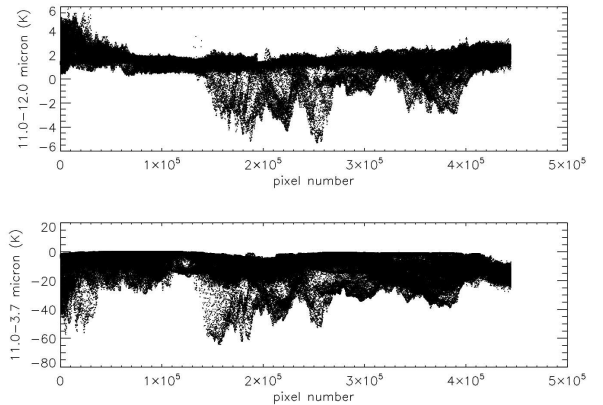


Figure 1: Top: Pixel values of $11\text{--}12\mu\text{m}$ test - negative values indicate possible volcanic ash. Bottom: Pixel values of $11\text{--}3.7\mu\text{m}$ test for same region

development of the ash flag.

There were three tests investigated as detailed in Section 2.1 to locate the ash with both the nadir and forward views being used. All of the following tests were applied over land or ocean. The first test uses the BT difference between $11.0\mu\text{m}$ and $12.0\mu\text{m}$. It was found that the forward view appeared to be more sensitive, particularly around the edges of the plume. After some refinement to the test, the pixel was considered to contain volcanic dust if:

$$BT_{11.0} - BT_{12.0} < -0.1 \quad (3)$$

This test located a relatively large amount of the volcanic ash plume and fig. 1 revealed few negative values apart from in the location of the ash. However while performing quite well in the control tests, it appeared that it may not be sufficient on its own.

The second test considers the BT difference between $3.7\mu\text{m}$ and $11.0\mu\text{m}$. Unlike the previous test, there is little indication in the literature of the value at which the threshold should be set. It was found that the $3.7\mu\text{m}$ channel would occasionally saturate at high BTs leading to invalid values in the data that would prevent the test from working. These invalid pixels were assigned the temperature at which the channel saturated since if the test gives a positive result, a BT higher than the saturation point will con-

tinue to give a positive result.

Images of the differences between these two channels were viewed and different thresholds were trialled to find a suitable limit that did not produce too many false readings but still located the majority of the ash. The ash plume was highlighted well but the values were not as distinct from some of the clouds, as may have been anticipated from Section 2.1. Fig. 1 shows the typical values of the test - regions of lower values correspond to pixels with negative results for the split-window test. Again, the forward view appeared more sensitive around the edges of the plume so it was used for this test. The pixel will be considered to contain volcanic dust if:

$$BT_{11.0} - BT_{3.7} < -20.0 \quad (4)$$

In the control tests, unacceptable numbers of pixels were falsely flagged. Trying to alter the threshold to increase the reliability tended to result in losing the ability to detect the ash successfully.

The third flag uses a combination of three tests, described in Section 2.1, that must all be satisfied in order for the pixel to be accepted as volcanic ash. Data for each part of the test was used from the nadir view. For a positive result:

$$B > 65 \text{ and } R_{0.66} < 10 \text{ or } NDVI < 0.1$$

where

$$B = 60 + 10 \cdot ((BT_{12.0} - BT_{11.0}) + (BT_{3.7} - BT_{11.0})) \quad (5)$$

More of the ash plume was flagged than for the previous two tests, as could be verified by studying the colour image. However, it did produce more false positives than the split-window test and would lose some sensitivity to the ash by altering the thresholds.

The split-window test, widely used in previous studies on ash detection, produced a good basis for a flagging system with the AATSR data considered here. However, to further reduce false results and maintain a relatively high number of ash pixels being correctly flagged, it was combined with the 11.0-3.7 μm test. The complete

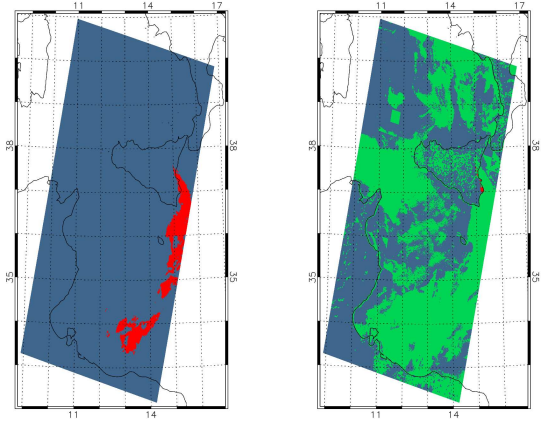


Figure 2: (L-R) Results of flag for volcanic ash; Results of cloud flag (green) overlaid on flag results (red)

flag recommended for volcanic ash is a combination of eq. 3 and eq. 4.

Fig. 2 shows the ash plume as detected by the final flag. In control tests, virtually no pixels were flagged in images of the dust or smoke and very few false readings appeared in other regions. Fig. 2 also displays the pixels classified as cloud (in green). There were two tests that were particularly responsible for flagging the ash as cloud. The first is a 11 μm spatial coherence test which produces a positive result for pixels displaying more variability than would be observed in clear conditions, which might be expected for the highly variable ash plume. The second test is a 11/12 μm view difference test (valid over the ocean) which uses the split-window difference in the nadir view to predict the same difference in the forward view, with clear sea pixels giving a correlation that the result is compared to. The ash has a distinct relationship in these two channels which would have contributed to this cloud flag being set.

3.2 Desert dust

To develop the desert dust flag, a large dust event was used where dust from the Sahara desert blew over Western Africa and out over the Atlantic. The event took place in March 2006 with dust becoming relatively dense over the land from around 07/03/2006 and then spreading west-

ward, reaching the coast around 09/03/2006-10/03/2006 and continuing further over the sea.

In order to gain a better idea of the location of the denser areas of dust, images of the Aerosol Optical Depth (AOD) obtained using data from the Multiangle Imaging SpectroRadiometer (MISR) and SEVIRI were used. MISR has a prior cloud flagging scheme reducing contamination from clouds in the retrieval. SEVIRI does not have any cloud removal process in place, however the retrieval tends to fail over cloud leading to the exclusion of contaminated pixels anyway. Areas of high AOD in the images using the different instruments thus indicate the possibility of a dense region of atmospheric aerosol. The current AOD retrieval from the AATSR data was also consulted – the cloud clearing removed much of the thicker dust regions but in conjunction with the MISR and SEVIRI retrievals, the gaps could be matched with dense areas of aerosol to locate the dust. A significant area of dust was located over the ocean around the region of 16°N , 22°W on 12/03/2006 which was used to construct the foundation of the flag then refinement was carried out with different images containing airborne dust and the control tests. It was discovered quite quickly that a flag developed for dust over the ocean would have to be adapted in order to work effectively over land so these two situations are discussed separately.

3.2.1 Dust over ocean

Tests found in the literature, as detailed in Section 2.2, were trialled first. Plots of the values of all the pixels for a test were used to gain insight into the variation across the dust cloud and typical values. The $11.0\text{-}12.0\mu\text{m}$ test was suggested to give a negative value in the presence of dust [10] however, over the ocean there were few negative values in any part of the image (fig. 3).

The $11.0\text{-}3.7\mu\text{m}$ test was also applied, with the forward view providing a clearer feature attributed to the dust. In the $11.0\mu\text{m}$ channel, the dust appeared warmer than much of the cloud and smaller differences between the $3.7\mu\text{m}$ channel were observed. A lower threshold was set on

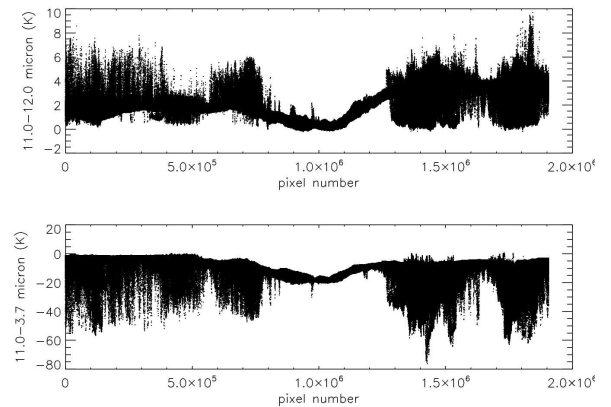


Figure 3: Top: Pixel values of the $11.0\text{-}12.0\mu\text{m}$ difference over the ocean. The narrowing of the range of values corresponds to the presence of dust. Bottom: Pixels values of $11.0\text{-}3.7\mu\text{m}$ test over dust. (Image from 12/03/2006)

this test in order to eliminate the colder cloud. When looking at the values of the test for all the pixels in the image, there was not an apparent range of values distinct from the regions not containing dust (fig. 3).

While the NDDI (as discussed in Section 2.2) could not be applied to the AATSR channels, a similarly constructed test using NDVI (eq. 2) was trialled instead. The dust appeared as a clearer feature in the nadir view from which a threshold was easier to set than in the forward view. A higher limit was set for this test since dust should remain in the lower, mostly negative values due to the slightly greater absorption expected at the shorter wavelength.

No single test isolated the dust successfully so with a combination of the three tests described above, the flag was applied to other regions of dust over the ocean. Compromises had to be made in order to ensure the detection of the plume in different images but in doing so, some residual cloud still remained. Difficulty in isolating the dust may be due to high levels of moisture reducing the spectral impact of the dust particles. Further tests were developed for the dust using knowledge of the properties of the particles. The plots of the pixel values for different tests could be used to discover whether the dust generally had a small range of values that could

make it distinguishable.

By using the characteristically large size of the dust particles, a ratio of the $0.55\mu\text{m}$ to $11.0\mu\text{m}$ channels was taken. The forward view was used due to the apparent increase in sensitivity to the edges of the plume of dust. The dust tended to have smaller values than other areas of the image due to the larger values of BT observed at $11.0\mu\text{m}$ than other particles in the atmosphere (as discussed in Section 2.2). Also, to reduce false readings further, the ratio of the $1.6\mu\text{m}$ and $11.0\mu\text{m}$ channels was introduced using similar reasoning.

After some more refinement of the thresholds for the different tests over the various images, the final flag gives a positive result for dust if all of the following conditions are satisfied:

$$BT_{11.0} - BT_{12.0} < 1.5 \quad (6)$$

$$BT_{11.0} - BT_{3.7} > -25.0 \quad (7)$$

$$\text{NDVI} < 0.0 \quad (8)$$

$$\frac{R_{0.55}}{BT_{11.0}} < 0.09 \quad (9)$$

$$\frac{R_{1.6}}{BT_{11.0}} < 0.09 \quad (10)$$

All of the tests above use the forward view apart from the NDVI (eq. 8).

Despite the combination of these tests, control tests revealed that there were still a few, mostly fairly isolated pixels falsely flagged, particularly in colder regions. The plots of pixel values for each test revealed that properties of the dust were generally uniform across most of the cloud. Having confirmed the low variability, a spatial coherence test was applied to the results from the spectral tests as suggested by [8]. Initially, the system using $27 \times 27 \text{ km}^2$ boxes, as detailed in Section 2.2, was used but this proved a very time consuming process when applied to the data and would not be practical when processing large numbers of orbits. An alternative method, the ‘‘opening test’’ [17], was found which took the results of the flag using only the spectral tests and ‘‘blurred’’ the pixels over an area set to 10×10 pixels. The blurred image is then compared to the original image and where the

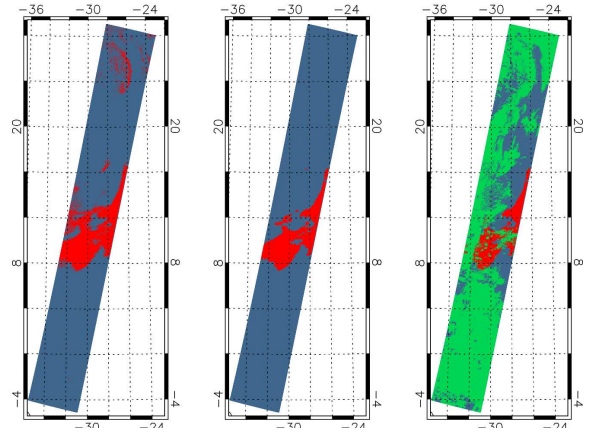


Figure 4: (L-R) Results of flag for dust with only spectral tests; Results for dust flag with spatial test; Results of cloud flag (green) overlaid on flag results (red) (Images from 11/03/2006)

difference in magnitude of a pixel is larger than a certain threshold, the pixel is determined to be cloudy and the flag is set to zero. Hence, isolated pixels blurred over the area will have low values compared to the original image and so will not produce a positive result.

With the inclusion of the spatial test, the dust flag appeared to work effectively over the water. Fig. 4 shows the effect of the spatial test and displays the extent of the cloud cover. Most frequently the $11/12\mu\text{m}$ view difference test was responsible for flagging the dust as cloud which, like the volcanic ash, may be because of the distinct impact of the dust in these channels. In the control testing, despite several thresholds set and the addition of the spatial test, high levels of false readings were still observed in the polar regions so latitude limits were also set so that no dust could be detected beyond $\pm 55^\circ$ latitude. The reason for this poor performance in colder areas, where there is often high amounts of cloud cover, might be partly due to the smaller contrasts in BTs at the longer wavelengths as well as lower values in the infrared channels.

3.2.2 Dust over land

The flag developed over the ocean was very ineffective at detecting the dust over the land. For instance, in the case where lofted dust was not present, large areas of the land over West Africa

gave negative values for the split window test, probably due to the dusty surface. As noted in [14], the contrast between land and blowing dust was less clear, making detection more difficult. The tests described for application over the ocean were investigated over the land with alterations made to the thresholds. No single test clearly isolated the dust while with combinations of tests the compromises made for detection in different images made it challenging to eliminate false positive results. Unfortunately, this issue persisted despite many refinements of the thresholds and investigation of further channel combinations such as the 0.66/11.0 μm ratio (which uses the impact of the dust in the infrared channels again). A satisfactory flag could not be produced for dust over land.

3.3 Smoke from biomass burning

The flag for smoke from biomass burning was developed using data from two events - one in Australia on 09/02/2009 around 35°S, 146°E and three images in Alaska on 16/08/2004, 17/08/2004 and 18/08/2004 around 65°N, 145°W. In Australia, conditions were very dry and hot while in Alaska, the fuel was boreal forest ignited after a particularly long dry, warm spell, though conditions would not have been as hot as Australia. The colour images of the regions and satellite photos for example from NASA^{1 2}, helped in confidence of the location of the smoke.

Some of the tests for the flag were constructed through adapting the method of Hutchison *et. al*, 2007 [12] where a ratio of a short wavelength to a much longer wavelength was taken. However, ratios between the visible channels and infrared channels highlighted the water/ice clouds but did not particularly bring out the feature of the smoke plumes. This may be explained by the particles starting to coalesce which may affect the impact in longer wavelengths.

¹NASA news article about Australian bush fire - <http://earthobservatory.nasa.gov/NaturalHazards/view.php?id=36979>

²NASA news article about Alaskan fire - <http://earthobservatory.nasa.gov/IOTD/view.php?id=4758>

As the ratios described above could not isolate the smoke further tests needed to be developed. Again using the concept that the smoke, due to the generally smaller size of the particles, scatters more light in the shorter wavelengths, tests were developed using the difference between the 0.55 μm and 1.6 μm channels and the 0.87 μm and 0.55 μm channels as a fraction of the 0.55 μm radiances.

To help eliminate clouds, two further tests were added using the BT difference between the 11.0 μm and 3.7 μm (where the smoke should have little influence in either channel leading to smaller differences) and the normalized split window difference (with the smoke again having small impact but highlighting the clouds).

After some refinement of the thresholds, a pixel would be flagged as containing smoke if:

$$\frac{(R_{0.55} - R_{1.6})}{R_{0.55}} < 0.6 \quad (11)$$

$$\frac{(R_{0.87} - R_{0.55})}{R_{0.55}} < 0.5 \quad (12)$$

$$\frac{R_{0.55}}{BT_{11.0}} > 0.06 \quad (13)$$

$$\frac{R_{0.87}}{BT_{11.0}} > 0.06 \quad (14)$$

$$\frac{(BT_{11.0} - BT_{12.0})}{(BT_{11.0} + BT_{12.0})} < 0.006 \quad (15)$$

$$BT_{11.0} - BT_{3.7} > -12.0 \quad (16)$$

All of the above tests use the forward view due to the increased sensitivity generally observed, particularly to the edges of the smoke plumes.

However, as with the dust flag over the ocean, there were still some remaining misidentified pixels despite the combination of the above tests. In order to reduce some of these residual incorrectly flagged pixels, a spatial test was employed (as suggested in [3]). The method of comparing the image of the results of the spectral tests to a “blurred” copy was used, as described for the dust in Section 3.2.1. Plumes of smoke tend to be smaller in their extent than the dust and are likely to be more variable so the pixels were blurred over a smaller area of 5 \times 5 pixels.

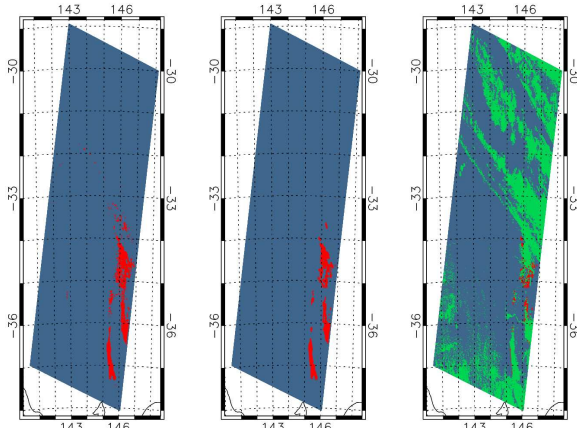


Figure 5: (L-R) Smoke in Australia (2 plumes) with only spectral tests; Smoke with spatial test included; Cloud cover (green) overlaid on pixels flagged as smoke (red)

The completed flag seemed to locate the smoke quite successfully in both locations (fig. 5). The cloud test primarily responsible for flagging the smoke as cloud was the visible channel test which uses two NDVI-like tests to categorise the surface type, including vegetation, desert and cloud [7]. In the control tests the flag did not work well over the water. Since only examples of smoke over land were used in its development, and having observed the difference in the testing techniques for dust over land or ocean, the flag has been restricted to use over land. More incorrect flagging was observed than in the case of the dust or volcanic ash during the control tests but in these few examples, often levels of around 0.2% of false positives were found which was decided to be acceptable. Further testing, in Section 4, provides greater insight into the levels of false readings.

4 Flag accuracy

To gain better insight into the level at which the flags are misidentifying pixels, all of the flags – volcanic ash over land and water, desert dust over water and smoke from biomass burning over land – were applied to large amounts of data. Fig. 6 shows the total number of times each pixel was flagged as volcanic ash during orbits from the first few days of May which include an eruption in Chile. Fig. 7 and fig. 8 similarly show the

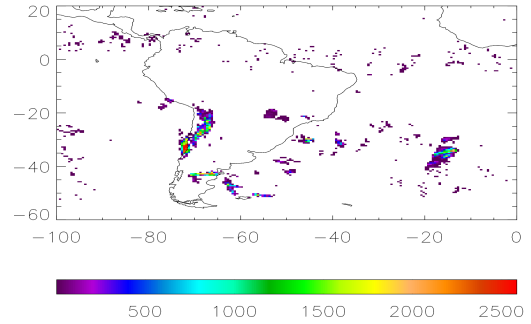


Figure 6: Results of volcanic flag for during the beginning of May over South America showing the total number of times each pixel was flagged

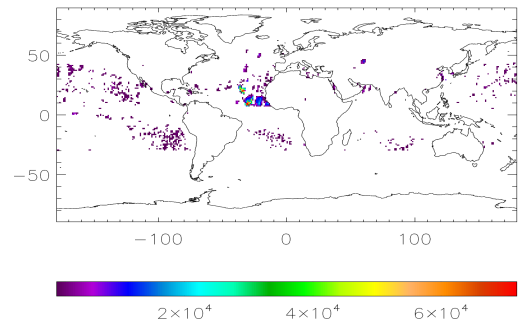


Figure 7: Results of dust flag for March 2006 showing the total number of times each pixel was flagged

results of the dust and smoke flags respectively applied to orbits throughout March 2006 during which time there was a large dust storm (used in development of the dust flag).

Across much of the globe, the volcanic ash produced few incorrectly flagged pixels and an eruption in Chile has been located, helping to confirm the use of the flag for different events. The flag was also applied for the March 2006 data where a large area around Korea and Mongolia was misidentified. There is no obvious explanation for the dense flagging in this region although it may be attributed to a particular surface type that happens to have similar properties as volcanic ash in the tests used. Low levels of misidentification are also seen in some of the far North in icy regions.

After only a few days had been processed the

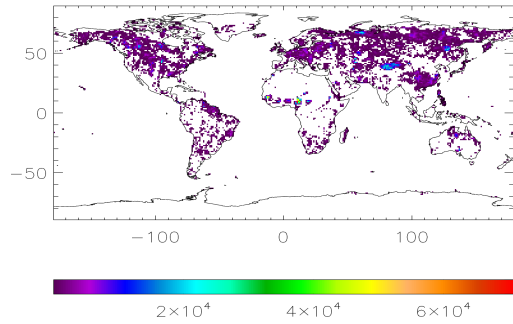


Figure 8: Results of smoke flag for March 2006 showing the total number of times each pixel was flagged

results were reviewed for any obvious problems with the flags. The dust flag appeared to densely flag a band around the globe at about -55°N . To correct this an extra condition was added to the dust flag which uses the generally higher temperature of the dust. To be flagged as positive the pixel must also satisfy:

$$BT_{11.0} > 275 \quad (17)$$

After this refinement, the dust flag appears to have performed quite successfully with very few falsely flagged pixels and the feature of the dust moving across the Atlantic clearly depicted (fig. 7).

Having observed in the limited control tests that the flag for smoke from biomass burning produced higher levels of incorrectly flagged pixels than the dust or ash flags, fig. 8 confirms a relatively large amount of misidentification. However, fig. 9 shows the fire activity as detected by AATSR which helps to support some of the positive flag results around Nigeria, Northern Brazil and possibly at some of the locations in North America and Russia.

5 Conclusions

5.1 Summary

The ORAC retrieval process analyses AATSR data to provide valuable information about the properties of aerosols and their effects in the atmosphere. However, the cloud clearing system

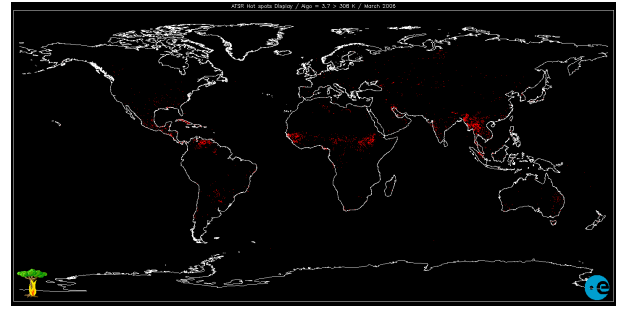


Figure 9: Image of fires detected by AATSR throughout March 2006

which aims to prevent contamination of the retrieval with water/ice clouds can also mistakenly remove large aerosol events. This project looked to develop individual flagging systems for volcanic ash, desert dust and smoke from biomass burning so that such events could be distinguished from cloud and included in the retrieval process. The type of aerosol flagged could also be incorporated into the *a priori* data.

To develop the flags, methods of detection from previous studies were researched and applied where possible to the AATSR data or used with some adaption. If tests from the literature were not sufficient then new tests were devised using the properties of the aerosol. In particular, the way in which the light was scattered, as determined by the size of the particle, and its composition, leading to any distinct absorption features was considered.

Three flags have been developed – volcanic ash over land and sea, desert dust over sea and smoke over land.

The volcanic ash flag used a combination of two tests that had been used in previous studies, confirming the BT difference between $11.0\mu\text{m}$ and $12.0\mu\text{m}$ as a successful test. Levels of falsely flagged pixels were generally low apart from around the region of Korea and Mongolia.

Use of negative results in the split-window test cloud not be used in identification of dust flag over water. However, with a revised threshold and in combination with other tests, the dust could be identified. A spatial test was also used in addition to the spectral channels. Very few false readings were produced, however it could not be used over land and a satisfactory flag for

use over land could not be developed within the limited time available for this study.

For the smoke flag, there were no tests in the literature that could be immediately applied to the AATSR data however, tests were based on some of the concepts behind the previously used methods and the properties of the aerosol were used in devising new tests. A spatial test was also used. Although much of the smoke seemed to be successfully detected, there were also higher levels of incorrectly flagged pixels (fig. 8). Some further refinement would be needed before the flag can be reliably used.

5.2 Further Work

The volcanic ash flag and dust flag may need some improvements, particularly in the case of the ash flag around Central/East Asia. Testing on different volcanic eruptions or dust events could also help confirm whether the flags are generally applicable. The smoke flag is not yet acceptable for use and will need more refinement to reduce the levels of false readings before it can be reliably applied.

Although a successful flag was not developed for dust over land promisingly, there were combinations of spectral channels that were highlighting the aerosol features. With more examples of dust events over land an acceptable flag might be produced. Also, detection of smoke over water could be investigated with appropriate images using techniques applied over land, although a new method may need to be developed.

Acknowledgement

The author would like to especially thank Dr. Thomas for all his interest and support in this project and for the provision of all the AATSR data.

References

- [1] D.T.L. Alexander, J.R. Anderson, and P.A. Crozier. Brown carbon spheres in East Asian outflow and their optical properties. *Science*, 321:833–836, 2008.
- [2] M.O. Andreae, G. Helas, K. Hungershofer, Y. Iinuma, R.S. Parmar, O. Schmid, T. Trautmann, J. Trentmann, A. Wiedensohler, and K. Zeromskiene. Modelling the optical properties of fresh biomass burning aerosol produced in a smoke chamber: results from the EFEU campaign. *Atmos. Chem. Phys.*, 8:3427–3439, 2008.
- [3] K. Asakuma, H. Kuze, N. Takeuchi, and T. Yahagi. Detection of biomass burning smoke in satellite images using texture analysis. *Atmospheric Environment*, 36:1531–1542, 2002.
- [4] I.J. Barton, A.R. Birks, M.C. Edwards, D. Llewellyn-Jones, C.T. Mutlow, and H. Tait. AATSR: Global-change and surface-temperature measurements from Envisat. Technical report, ESA, Feb 2001.
- [5] K.M. Bedka, S.T. Bedka, T.A. Berendes, B. Bernstein, W.F. Feltz, J. Haggerty, D.B. Johnson, J.R. Mecikalski, P. Minnis, J.J. Murray, M. Pavikibus, E. Williams, and A.J. Wimmers. Aviation applications for satellite-based observations of cloud properties, convection initiation, in-flight icing, turbulence, and volcanic ash. *Bulletin of the American Meteorological Society*, 88, 2007.
- [6] A. Birks, ESA, VEGA Group PLC, and University of Leicester. *AATSR Product Handbook*. ESA, 2.2 edition, Feb 2007.
- [7] A. R. Birks. *AATSR Technical Note: Improvements to the AATSR IPF relating to Land Surface Temperature Retrieval and Cloud Clearing over Land*. Science and Technology Facilities Council; Rutherford Appleton Laboratory, Sept 2007.
- [8] H.E Brindley and J.E Russell. Improving GERB scene identification using SEVIRI: Infrared dust detection strategy. *Remote Sensing of Environment*, 104:426–446, 2006.
- [9] B. Connell. Volcanic ash/aerosol and dust. http://rammb.cira.colostate.edu/wmovl/vrl/pptLectures/natural_hazards/volcano/ash_dust.ppt, 2003.

- [10] B.H. Connell and F.J. Prata. Detecting volcanic ash and blowing dust using GEOS, MODIS and AIRS imagery. ams.confex.com/ams/pdfpapers/100112.pdf.
- [11] P.R. Field, O. Möhler, P. Connolly, M. Krämer, R. Cotton, A.J. Heymsfield, H. Saathoff, and M. Schnaiter. Some ice nucleation characteristics of Asian and Saharan desert dust. *Atmos. Chem. Phys.*, 6, 2006.
- [12] K.D. Hutchison, B.D. Iisager, and J.M. Jackson. Differentiating between clouds and aerosol during the NPOESS era. In *Third Symposium on Future National Operational Environmental Satellites*. American Meteorological Society, 2007.
- [13] I. Koren. On the importance of locality when estimating the aerosol effects on climate. *Scitizen*, 2006.
- [14] S. Miller. *MODIS Dust Enhanced Product - Focus Tutorial*. NRL Monterey, Marine Meteorology Division, http://www.nrlmry.navy.mil/sat_training/dust/modis/index.html - last updated: 2003.
- [15] Parliamentary Office of Science and Technology. Climate change science (Postnote). Technical report, 2007.
- [16] A.J. Prata. Observations of volcanic ash clouds in the 10-12 μ m window using AVHRR/2 data. *International Journal of Remote Sensing*, 10(4-5):751–761, 1989.
- [17] D. Ramon. Validation of the MERIS land data products: Validation of the aerosol level 3 product. In *Final report for the ESTEC Contract*, 2006.
- [18] G.E. Thomas, E. Carboni, A.M. Sayer, C.A. Poulsen, R. Siddans, and R.G. Grainger. Oxford-RAL aerosol and cloud (ORAC): Aerosol retrievals from satellite radiometers. In *Aerosol Remote Sensing Over Land*. Springer, 2009.

Appendix A

Satellites provide an efficient way of collecting large amounts of data from across the globe in a regular and reliable way. They allow large events to be tracked by day and night and remote regions of Earth can be covered. Envisat, a polar orbiting satellite launched in 2002, carries the Advanced Along Track Scanning Radiometer (AATSR) which was primarily designed to retrieve sea surface temperatures. It was also designed to work along side the previous generation Along Track Scanning Radiometer, ATSR-2, which was launched in 1995 on the ERS-2 satellite. However, ATSR-2 has recently ceased operation. The two instruments provided virtually identical measurements and were functionally very similar.

The dual view of the instruments allows much easier separation of the surface and atmospheric contributions to the radiance at the top of the atmosphere than a single view. The forward view may also offer increased sensitivity to the atmosphere than might be seen in the nadir view. Images can be produced with 1 km spatial resolution with a swath width of 512 km. Envisat achieves global coverage around every three days with a track over the surface that repeats around every 35 days.

AATSR has two onboard, thermally controlled black bodies in the infrared range allowing the instrument to be self-calibrating in the infrared region channels. For the visible channels, further calibration is carried out using a view of the sun. The main advantage of AATSR over the older ATSR-2 is that there are fewer restrictions on the telemetry of the visible data, allowing more to be collected.

Appendix B

The ORAC retrieval employs an optimal estimation retrieval scheme - an iterative process which fits values of aerosol scattering and absorption, gas absorption and models of the surface reflectance in such a way to model the observed radiance.

Before the retrieval can be made, the removal of cloud is carried out to prevent contamination of the results. There are 12 tests for cloud of which only one needs to be set to indicate the presence of cloud (more detail about the flags can be found in [6] and [7]). The clearing over sea is applied very conservatively to prevent contamination in sea surface temperatures. However, it would be very difficult to eliminate all misidentifications of pixels, both over land and sea.

It is worth noting that flags produced in the empirical way used in this investigation cannot detect the relevant aerosol to a reasonable degree of success without misidentification of pixels also occurring. However, particularly in the case of more isolated pixels, if the incorrect aerosol type is included in the *a priori* data the iterative process of the retrieval should recognise the poor fit to the observations and reject the *a priori* information.